

Complexation of metal ions with the novel diazadithia crown ethers carrying two pyrene pendants in acetonitrile-tetrahydrofuran

Ümmühan Ocak · Miraç Ocak · Aysel Başoğlu · Semanur Parlayan · Hakan Alp · Halit Kantekin

Received: 16 June 2009 / Accepted: 6 August 2009 / Published online: 19 August 2009
© Springer Science+Business Media B.V. 2009

Abstract Two crown ethers carrying pyrene side arms with nitrogen-sulfur donor atom were designed and synthesized by the reaction of the corresponding macrocyclic compounds and 1-bromomethyl-pyrene. The influence of metal cations such as Al^{3+} , Zn^{2+} , Fe^{2+} , Fe^{3+} , Co^{2+} , Ni^{2+} , Mn^{2+} , Cu^{2+} , Cd^{2+} , Hg^{2+} and Pb^{2+} on the spectroscopic properties of the ligands was investigated in acetonitrile-tetrahydrofuran (1:1) by means of absorption and emission spectrometry. Absorption spectra show isosbestic points in the spectrophotometric titration of Al^{3+} , Zn^{2+} , Fe^{2+} , Ni^{2+} , Cu^{2+} , and Pb^{2+} with 16-membered crown ether. Similar results were obtained for Al^{3+} , Fe^{2+} , Hg^{2+} , Cu^{2+} and Pb^{2+} with 14-membered crown ether. The results of spectrophotometric titration experiments disclosed the complexation stoichiometry and complex stability constants of the novel ligands with these cations. According to spectrofluorimetric titration measurements the 14-membered diazadithia crown ether showed sensitivity for Pb^{2+} with linear range and detection limit of 1.3×10^{-6} to 5.2×10^{-5} M and 5.2×10^{-7} M, respectively. The 16-membered diazadithia crown ether showed sensitivity for Ni^{2+} with linear range and detection limit of 1.3×10^{-7} to 5.2×10^{-6} M and 4.1×10^{-8} M, respectively.

Keywords Crown ether · Diazadithia donor atom · 1-bromomethyl-pyrene · Fluorescence spectroscopy · Stability constant · Metal cation

Introduction

Crown ethers discovered by Pedersen have been used in the design of new chemosensors based on their unique ability to bind metal cations sensitively and selectively [1–5]. Oxygen donor atom carrying crown ethers shows affinity to alkali and alkaline earth metal cations while nitrogen and sulfur donor atoms carrying crown ethers are sensitive for soft metal cations Cd^{2+} , Pb^{2+} , Ag^+ , Cu^{2+} and Hg^{2+} [6, 7]. The detection of these cations in various media such as biological material and environmental systems is particularly important because of their toxic properties.

Fluorescent chemosensors are of great interest because of their selectivity and sensitivity for the desired chemical species [8–10]. Fluoroionophores consisting of a recognition part (ionophore) and a signaling part (fluorophore) have been used to determine various cations. Such molecular cation sensor has to bind desired cation selectively among the other cations. On the other hand, the signaling part is important for sensitivity of the sensor.

Recently, fluorescent macrocyclic ligands having a simple spacer such as methylene group, connecting the binding part and the signaling part, have been synthesized [11, 12]. “Fluorophore-spacer-receptor” systems have many advantages in monitoring the interaction of cation-macrocycle. Upon cation binding the fluorescence intensity of the fluorophore group may increase or decrease. On the other hand, during the interaction of a fluorescent sensor with the metal cation a red or blue shift in the absorption and/or fluorescence spectra

Ü. Ocak (✉) · M. Ocak · S. Parlayan · H. Kantekin
Department of Chemistry, Faculty of Arts and Sciences,
Karadeniz Technical University, 61080 Trabzon, Turkey
e-mail: ummuhanocak@yahoo.com

A. Başoğlu
Bayburt University, Vocational School, Bayburt, Turkey

H. Alp
Karadeniz Technical University, Maçka Vocational School,
Maçka, Trabzon, Turkey

can be observed. Such photo-physical changes have been explained with photoinduced charge transfer (PCT), photoinduced electron transfer (PET) or excimer or exciplex emission [13]. PET has been explored extensively in the presence of metal cations in solution [14–16].

Pyrene and its derivatives have been used as signaling groups in the design of fluorescent cation chemosensors [17–19]. These groups have been shown to have very interesting photo-physical properties. Fluorescent chemosensors carrying pyrenyl-aza crown ether were developed to determine metal cations. Such investigations also reveal the complexation properties of the ligand with the cation. Upon complexation, the chelation enhanced fluorescence (CHEF) or chelation enhanced quenching (CHEQ) are observed for these systems [20–22].

In the present study we report the preparation of two 14- and 16-membered diazadithia crown ether ligands having two pyrenyl sidearms, and present the complexation properties of the ligands with a series of metal cations. Our aim was to reveal the effect of crown cavity size of new fluorescent ligands on the cation complexation properties such as complex composition and complex stability constant. Complex stability constant is an important parameter to disclose the effectiveness of ligand in cation binding. Therefore, we calculated the complex stability constants and complex compositions of metal cations with the ligands by using spectrophotometric titrations in acetonitrile-tetrahydrofuran solution (1:1). We propose 14-membered fluorescent ligand and 16-membered ligand for lead and nickel determination, respectively.

Experimental

Chemicals

Acetonitrile and tetrahydrofuran from Merck (spectrometric grade) were the solvents for absorption and fluorescence measurements. All metal perchlorates purchased from Acros were of the highest quality available and vacuum dried over blue silicagel before use.

Apparatus

¹H NMR spectra were recorded on a Varian 200 A spectrometer, using CDCl₃ with TMS as the internal reference. IR spectra were recorded on a Perkin-Elmer 1600 FTIR spectrophotometer using KBr pellets. Elemental analysis was performed on Costech 4010 CHNS instrument. The absorption spectra of the solutions were recorded using a Thermo Evolution 60 model spectrophotometer. A Photon Technologies International Quanta Master Spectroflu-

rimeter (model QM-4/2006) was used for all fluorescence measurements.

Measurements

Stock solutions of the ligands were prepared in tetrahydrofuran and the ligand solutions used for titrations were prepared from these solutions by dilution. Absorption spectra of the ligands in acetonitrile-tetrahydrofuran (1:1) containing 10 molar equivalents of Al³⁺, Zn²⁺, Fe²⁺, Fe³⁺, Co²⁺, Ni²⁺, Mn²⁺, Cu²⁺, Cd²⁺, Hg²⁺ and Pb²⁺ cations were measured using 1-cm absorption cell. The concentration of each ligand was 1.3 × 10⁻⁵ M in these measurements and this ligand concentration was used in the spectrophotometric titrations. Fluorescence spectra of the ligands in acetonitrile-tetrahydrofuran (1:1) containing 10 molar equivalents of Al³⁺, Zn²⁺, Fe²⁺, Fe³⁺, Co²⁺, Ni²⁺, Mn²⁺, Cu²⁺, Cd²⁺, Hg²⁺ and Pb²⁺ cations were measured using 1-cm quartz cell. The concentrations of ligands, L(1) and L(2) for fluorescence measurements were 1.3 × 10⁻⁷ M and 1.3 × 10⁻⁸ M, respectively, and the excitation wavelength was 345 nm for the ligands. Fluorescence emission spectra were recorded in the range 370–450 nm with slit width 1.0 nm.

The stoichiometry of the complexes was determined by using the molar-ratio method from the data of spectrophotometric titrations. The stability constants were calculated according to the procedure described in the literature [23].

Synthesis

Synthesis of (3)

1-Pyrene methanol (2.25 g, 9.69 mmol) and PBr₃ (1.05 g, 3.86 mmol) were refluxed in benzene (125 mL) for 4 h. The reaction was monitored by TLC (silica gel, dichloromethane). The solution was extracted with diethyl ether:water (3:2) mixture, rinsed with water twice, and dried over anhydrous magnesium sulfate. The solvent was then removed under reduced pressure to yield 1-bromomethyl-pyrene as a pale yellow solid. Yield (92.6%), m.p: 140–142 °C. ¹H NMR (CDCl₃): (δ) 5.14 (s, 2H), 8.00–8.28 (m, 9H).

Synthesis of L(1)

Compound (1) [24] (0.09 g, 0.28 mmol) and 1-bromomethyl-pyrene (3) (0.50 g, 1.69 mmol) were dissolved in 100 mL of tetrahydrofuran:toluene (1:1) and purged under nitrogen atmosphere in a Schlenk system connected to a vacuum line. Triethylamine (1.01 g, 9.95 mmol) was

added dropwise to this solution. The reaction mixture was refluxed and stirred at reflux temperature for 30 h, monitored by TLC [silica gel (n hexane:ethyl acetate) (1:1)]. At the end of this period, the reaction mixture was filtered. The filtrate was concentrated on an evaporator to 10 mL and the solid formed was filtered off, then dried *in vacuo*. A yellow solid product (yield 62.2%) was obtained by recrystallization from ethanol-THF, mp 238–240 °C. Anal. Calc. for C₅₂H₄₂N₂S₂: C, 82.28; H, 5.58; N, 3.69; S, 8.45%. Found: C, 82.15; H, 5.95; N, 3.52; S, 8.20%. IR (KBr disc, cm⁻¹): 3037 (Ar-H), 2917–2803 (C-H), ¹H-NMR (CDCl₃): (δ) 6.93–7.30 (m, 8H, macrocyclic Ar-H), 7.98–8.66 (m, 18H, pyrene Ar-H), 4.14 (s, 4H, pyrene-CH₂), 3.80 (s, 4H, benzene-CH₂), 3.00–3.08 (m, 4H, N-CH₂), 2.71–2.79 (m, 4H, S-CH₂). MS (EI): *m/z* = 759.22 [M]⁺.

Synthesis of L(2)

L(2) was prepared from compound **(2)** [24] (0.22 g, 0.61 mmol) and 1-bromomethyl-pyrene (**3**) (1.06 g, 3.62 mmol) in 71.2% yield by a method similar to that used for **L(1)**. The reaction mixture was refluxed and stirred at reflux temperature for 60 h. A yellow solid product was obtained by washing with hot acetone, mp 216–218 °C. Anal. Calc. for C₅₄H₄₆N₂S₂: C, 82.40; H, 5.89; N, 3.56; S, 8.15%. Found: C, 82.34; H, 5.73; N, 3.81; S, 8.52%. IR (KBr disc, cm⁻¹): 3040 (Ar-H), 2928–2795 (C-H), ¹H-NMR (CDCl₃): (δ) 6.86–7.26 (m, 8H, macrocyclic Ar-H), 8.01–8.44 (m, 18H, pyrene Ar-H), 4.26 (s, 4H, pyrene-CH₂), 3.79 (s, 4H, benzene-CH₂), 2.69–2.73 (m, 8H, N-CH₂ and S-CH₂), 1.91 (m, 4H, C-CH₂-C), MS (EI): *m/z* = 787.33 [M]⁺.

Results and discussion

Characterization of the ligands

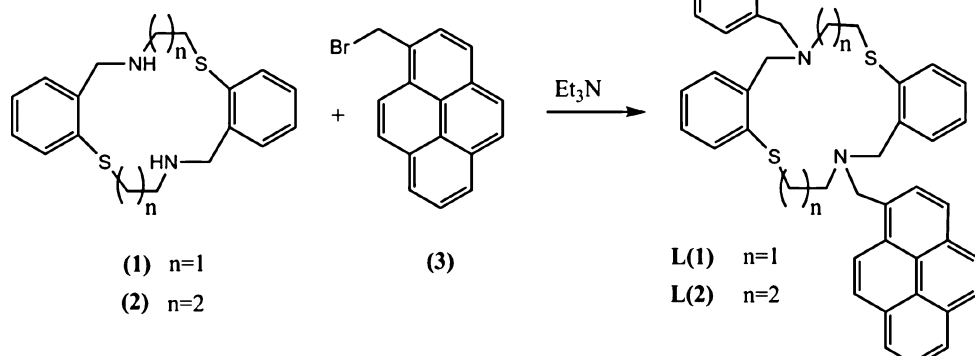
The synthetic pathway to new ligands **L(1)** and **L(2)** is summarized in Scheme 1. Compounds **(1)** and **(2)** were prepared according to the literature [24].

L(1) and **L(2)** were synthesized by the reaction of the corresponding macrocyclic compounds with 1-bromomethyl-pyrene (**3**) in tetrahydrofuran:toluene (1:1). The absence of the secondary amine band pertaining to the starting materials in the IR spectra of the ligands with pyrene side arm has supported the structures. In the ¹H-NMR spectrum of ligands, **L(1)** and **L(2)** the singlets (4H) belonging to the methylene protons of pyrenyl groups were observed at δ = 4.14 and δ = 4.26 ppm, respectively. In the ¹H-NMR spectrum of **L(2)**, the multiplet at δ = 1.91 ppm (4H) belongs to C-CH₂-C protons. On the other hand, the mass spectral analysis of the ligands confirms the proposed structures.

Absorption spectra

The absorption spectra of the ligands in acetonitrile-THF (1:1) display the strong $\pi-\pi^*$ absorption bands at 300–360 nm characteristic of the pendant pyrenyl groups (Figs. 1 and 2). As seen from Fig. 1, **L(1)** possesses three absorption bands at 314, 328 and 344 nm and the molar absorption coefficients are 2.0×10^4 , 4.9×10^4 , 7.2×10^4 cm⁻¹ M⁻¹, respectively. **L(2)** (see Fig. 2) also possesses three absorption bands at the same wavelengths where the molar absorption coefficients are 1.9×10^4 , 4.6×10^4 , 6.5×10^4 cm⁻¹ M⁻¹.

Scheme 1 Synthetic pathway to the new macrocyclic ligands **L(1)** and **L(2)** used in this study



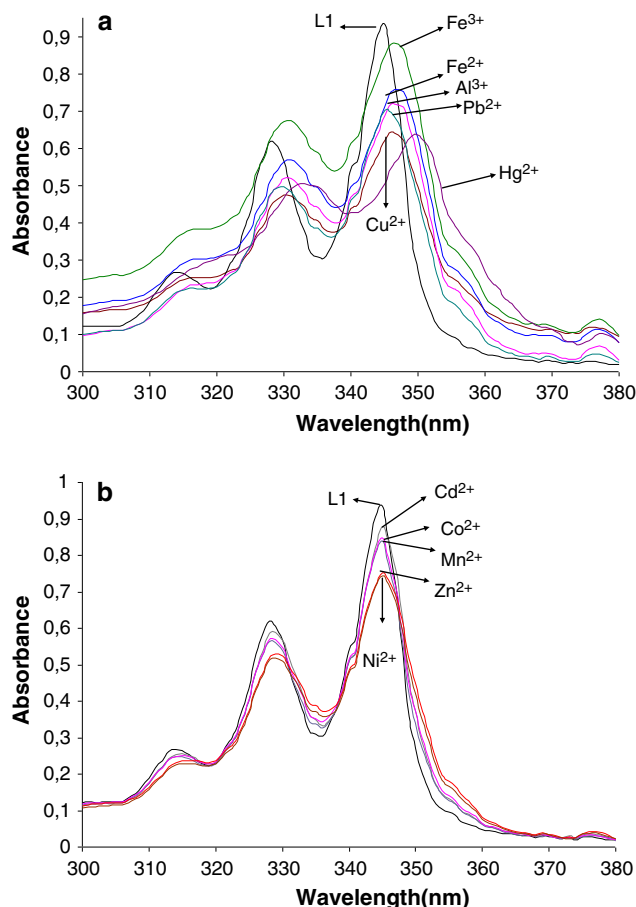


Fig. 1 The effect of metal cations on the absorption spectra of the ligand (**1**) in acetonitrile-tetrahydrofuran solution (1/1). Ligand concentration = 1.3×10^{-5} M. Metal perchlorate concentrations = 1.3×10^{-4} M. **a** for Al³⁺, Fe²⁺, Fe³⁺, Cu²⁺, Hg²⁺ and Pb²⁺. **b** for Zn²⁺, Co²⁺, Ni²⁺, Mn²⁺ and Cd²⁺

Figure 1a shows the effect of 10 equivalent excess of metal concentrations on the absorption spectra of the ligand **L(1)**. The red shifts at all the absorption bands and absorbance decreases at 344 nm are pronounced. Spectrophotometric titration results show that these cations formed stable complexes with **L(1)** except for Fe³⁺. The most significant red shift was observed for Hg²⁺. As seen from Table 1, Hg²⁺ formed the most stable complex (the log *K* value was 4.92 for Hg²⁺-**L(1)** complex) among the cations with this ligand. Cu²⁺, Hg²⁺, Pb²⁺, Al³⁺, Fe²⁺ and Fe³⁺ ions caused a new broad absorption band at 376 nm. These results show that these ions interact with pyrene groups of the ligand (**1**).

The presence of 10 equivalents of Cd²⁺, Co²⁺, Ni²⁺, Zn²⁺ and Mn²⁺ cations caused a decrease of absorption at 314, 328 and 344 nm (Fig. 1b). The decrease was less pronounced for Cd²⁺, Co²⁺ and Mn²⁺ cations with respect to Ni²⁺ and Zn²⁺. However, a stable complex formation was not observed for the cations in the spectrophotometric titration experiments.

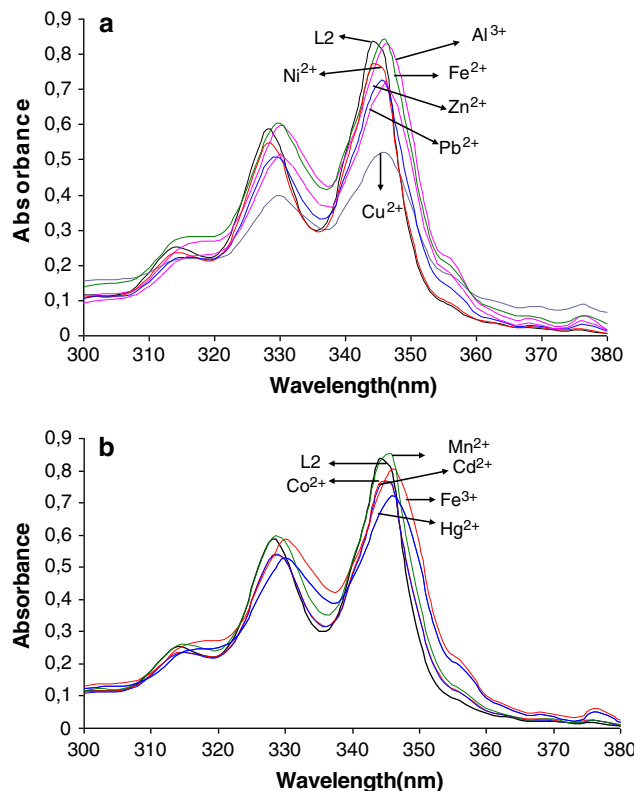


Fig. 2 The effect of metal cations on the absorption spectra of the ligand (**2**) in acetonitrile-tetrahydrofuran solution (1/1). Ligand concentration = 1.3×10^{-5} M. Metal perchlorate concentrations = 1.3×10^{-4} M. **a** for Al³⁺, Ni²⁺, Fe²⁺, Zn²⁺, Pb²⁺ and Cu²⁺. **b** for Hg²⁺, Co²⁺, Mn²⁺, Cd²⁺ and Fe³⁺

Figure 2 shows the effects of excess metal concentrations in the absorption spectra of **L(2)**. As seen from Fig. 2a, the presence of 10 equivalents of Cu²⁺, Zn²⁺, Pb²⁺, Al³⁺, Fe²⁺ and Ni²⁺ ions cations caused a decrease of absorption at 314, 328 and 344 nm except for Al³⁺ and Fe²⁺. Especially, Cu²⁺ cation produces a pronounced decrease in the absorbance at 328 and 344 nm. The red shifts at all the absorption bands observed were similar to that of **L(1)**. There was a regular relationship between the red shift value and the stability constant also for this ligand. As seen from Table 1, among the complexes of **L(2)**, the least stable complex was Ni²⁺-**L(2)** complex with a log *K* value of 3.87 and Ni²⁺ caused the least red shift among the cations (see Fig. 2a). A stable complex formation was not observed for Cd²⁺, Co²⁺, Hg²⁺, Fe³⁺ and Mn²⁺ cations in the spectrophotometric titration experiments. However, the excess of these metal cations also caused a little red shift in all the absorption bands except for Co²⁺ (Fig. 2b).

Spectrophotometric titrations with **L(1)**

Al³⁺, Zn²⁺, Fe²⁺, Fe³⁺, Co²⁺, Ni²⁺, Mn²⁺, Cu²⁺, Cd²⁺, Hg²⁺ and Pb²⁺ cations were used in the spectrophotometric

Table 1 Complex stability constants and complex composition of ligands **L(1)** and **L(2)** with metal cations in acetonitrile-tetrahydrofuran (1:1) obtained by spectrophotometric titrations

Cation	Complex composition ^a (M:L)		Stability constant ^a (Log K)	
	L(1)	L(2)	L(1)	L(2)
Cu ²⁺	2:1	2:1	4.11 ± 0.73	4.40 ± 0.32
Hg ²⁺	2:1	–	4.92 ± 0.34	–
Zn ²⁺	–	1:1	–	4.55 ± 0.41
Al ³⁺	1:1	1:1	4.61 ± 0.25	4.56 ± 0.43
Fe ²⁺	1:1	1:1	3.79 ± 0.65	4.52 ± 0.07
Pb ²⁺	1:1	1:1	4.37 ± 0.35	4.67 ± 0.17
Ni ²⁺	–	2:1	–	3.87 ± 0.88

^a The average values calculated from the data obtained from three independent absorbance measurements

titration experiments with **L(1)**. In the absorption spectra of **L(1)**, regular changes and many isosbestic points were observed with increasing concentrations of Al³⁺, Cu²⁺, Fe²⁺, Hg²⁺ and Pb²⁺. There was no regular change in the absorption spectra for the other tested metal cations.

Figure 3 shows the effect of increasing concentrations of Al³⁺ on the absorption spectra of **L(1)** in which five isosbestic points are observed at 318, 322, 330, 338 and 348 nm, indicating the presence of many equilibria in the solution. One of them may belong to the complex formation equilibria between Al³⁺ and **L(1)**. Regular absorbance decreases were detected at 314, 328 and 344 nm with increasing concentrations of Al³⁺. On the other hand, a red shift was observed at all absorption bands. Apparently, there was also regular absorbance increase at 376 nm during the complexation and hence we confirmed the 1:1 complex composition from this. The decrease of absorbance at 344 and 328 nm provided the determination of the complex composition of Al³⁺–**L(1)**. The inflection

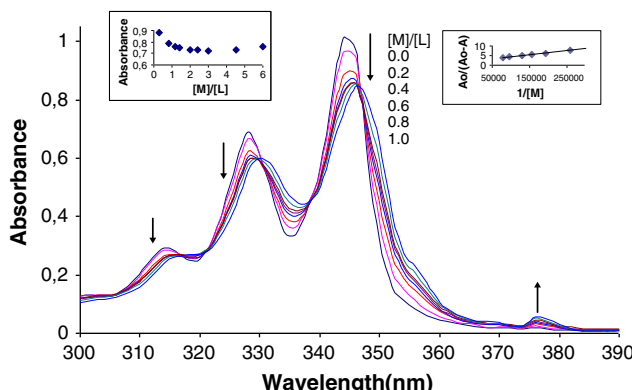


Fig. 3 The variation of absorbance of **L(1)** with the concentration of Al³⁺, added as 0–1 equivalent of Al(ClO₄)₃. Ligand concentration: 1.3 × 10⁻⁵ M. Inset: Measurements were carried out at 344 nm

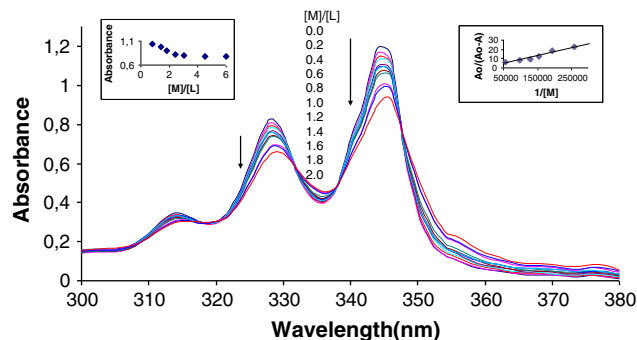


Fig. 4 The variation of the absorbance of **L(1)** with the concentration of Cu²⁺, added as 0–2.0 equivalents of Cu(ClO₄)₂. Ligand concentration: 1.3 × 10⁻⁵ M. Insets: Measurements were carried out at 344 nm

point was 1.0 ([M]/[L]) in the molar ratio plot [see Fig. 3 (inset left)]. Thus, it can be concluded that **L(1)** formed a stable 1:1 (M:L) complex with Al³⁺. Similar spectrophotometric titration curves were obtained for Pb²⁺ and Fe²⁺ with **L(1)** and the complex composition was also 1:1 for these cations (Table 1).

Cu²⁺ and Hg²⁺ cations formed the 2:1 (M:L) complex with 14-membered crown ether **L(1)** and there were also three and two isosbestic points in the absorption spectra in the titration of Cu²⁺ and Hg²⁺, respectively. Figure 4 shows the changes in the absorption spectra of **L(1)** with increasing concentrations of Cu²⁺. A regular absorbance change was observed in the spectra at 328 and 344 nm and the decreases of absorbance at both wavelengths provided the determination of the complex composition of Cu²⁺–**L(1)**. As seen from Fig. 4 (inset left), the inflection point was 2.0 ([M]/[L]). It can thus be concluded that **L(1)** formed a 2:1 (M:L) stable complex with Cu²⁺ by **L(1)**. We obtained similar spectrophotometric titration curves for Hg²⁺ with **L(1)** and the complex composition was also 2:1(M:L) for this cation (Table 1).

Spectrophotometric titrations with **L(2)**

The same cations were used in the spectrophotometric titration experiments with **L(2)**. Regular changes and many isosbestic points similar to those of **L(1)** were observed in the absorption spectra of **L(2)** with increasing concentrations of Al³⁺, Zn²⁺, Fe²⁺, Ni²⁺, Cu²⁺ and Pb²⁺.

L(2), a 16-membered crown ether, formed stable 1:1 (M:L) complexes with Al³⁺, Fe²⁺, Pb²⁺ and Zn²⁺. Figure 5 shows the effect of increasing concentrations of Pb²⁺ cation on the absorption spectra of **L(2)**. Many isosbestic points are observed in the spectra, implying the existence of many equilibria in the solution. Regular absorbance decreases were detected at 276, 328 and 344 nm with increasing concentrations of Pb²⁺. On the

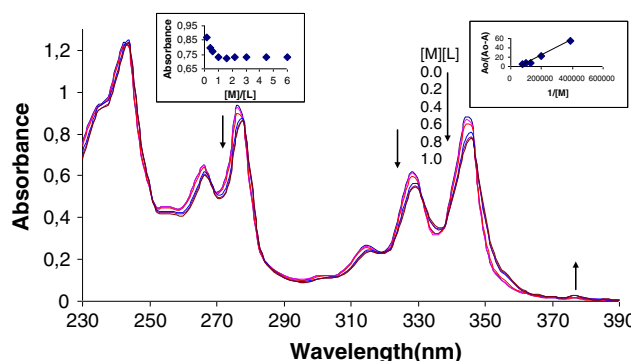


Fig. 5 The variation of the absorbance of **L(2)** with the concentration of Pb^{2+} , added as 0–1 equivalent of $\text{Pb}(\text{ClO}_4)_2$. Ligand concentration: 1.3×10^{-5} M. Insets: Measurements were carried out at 344 nm

other hand, a red shift was observed at all absorption bands. During the complexation, a regular absorbance increase was detected at 376 nm from which we confirmed the 1:1 complex composition. The decrease of absorbance at 344 nm provided the determination of the complex composition of $\text{Pb}^{2+}\text{--L}(2)$. As seen from Fig. 5 (inset left), the inflection point was 1.0 ($[\text{M}]/[\text{L}]$) in the molar ratio plot. Thus, it can be concluded that **L(2)** formed a stable 1:1 (M:L) complex with Pb^{2+} . We obtained similar spectrophotometric titration curves for Al^{3+} , Fe^{2+} , Zn^{2+} and Cu^{2+} with **L(2)**. The complex composition was 1:1 for Al^{3+} , Fe^{2+} and Zn^{2+} cations while the complex composition was 2:1(M:L) for Cu^{2+} (Table 1).

The effect of increasing concentrations of Ni^{2+} on the absorption spectra of 16-membered crown ether **L(2)** is different from those of other metal cations (see Fig. 6). A pronounced absorbance increase was observed in the spectra between 230 and 310 nm. In addition to this, we observed absorbance decreases at 344 nm belonging to the pyrene groups as similar to those of other titrations. The increase in absorbance at 276 nm provided the

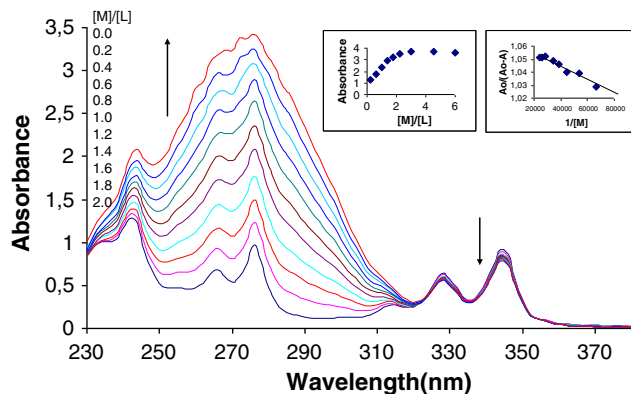


Fig. 6 The variation of the absorbance of **L(2)** with the concentration of Ni^{2+} , added as 0–2.0 equivalents of $\text{Ni}(\text{ClO}_4)_2$. Ligand concentration: 1.3×10^{-5} M. Insets: Measurements were carried out at 276 nm

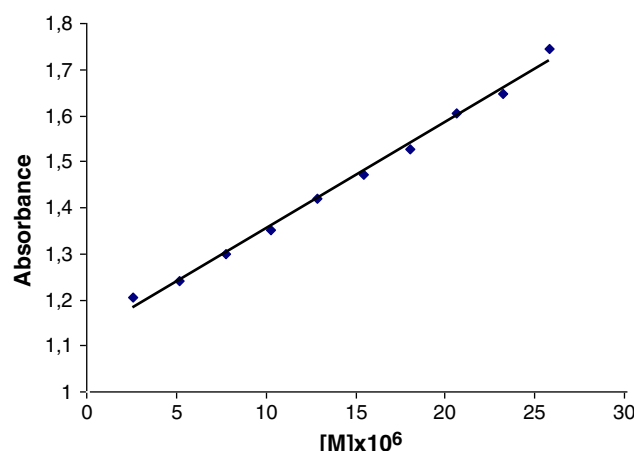


Fig. 7 The absorbance of **L(2)** versus Ni^{2+} concentration for the spectrophotometric titration. Wavelength: 240 nm, Ligand concentration = 1.3×10^{-5} M

determination of the complex composition of $\text{Ni}^{2+}\text{--L}(2)$ and the inflection point was 2.0 ($[\text{M}]/[\text{L}]$) [see Fig. 6 (inset left)]. It can thus be concluded that **L(2)** formed a 2:1 (M:L) stable complex with Ni^{2+} by **L(2)**. A single isobestic point was observed at 324 nm for this cation and this shows the presence of one equilibrium in the solution and hence, the formation of the $\text{Ni}^{2+}\text{--L}(2)$ complex.

A regular absorbance increase was detected for Ni^{2+} in the spectrophotometric titration with **L(2)** at 240 and 314 nm. A linear response of the absorbance as a function of Ni^{2+} concentration at both wavelengths was observed from 2.6×10^{-6} to 7.7×10^{-5} M. However, the calibration sensitivity was higher at 240 nm and $R^2 = 0.9993$ was found for the calibration graph at 240 nm (Fig. 7).

In order to determine the complex stability constant, the ratio of $A_o/(A_o - A)$ was plotted versus $1/[M]$ which gave a good straight line. A_o and A are the absorbance of the free ligand and the absorbance of the solution containing the cation, respectively. The stability constant was calculated from the ratio intercept/slope [23]. Corresponding plots can be seen in Figs. 3, 4, 5, 6 (insets).

Table 1 shows complex stability constants and complex composition of the ligands with metal cations in acetonitrile-THF(1:1), obtained from spectrophotometric titrations. Apparently, the most stable complex was obtained with **L(1)** for Hg^{2+} . The complex composition was 2:1(M:L) in this case. It is interesting that Hg^{2+} does not form a stable complex with 16-membered crown ether **L(2)**. Cu^{2+} formed the 2:1 (M:L) complex with both ligands (see Table 1). This result shows that the size of the crown cavity is not important over the complexation composition for Cu^{2+} . We obtained similar results for Al^{3+} , Fe^{2+} and Pb^{2+} . However, these cations form the 1:1 complex for both ligands. This result shows that metal cation type is important in the complex composition. Also,

“ion-cavity size match” may be effective in the complexation with these ligands. As known “ion-cavity size match” concept is valid in the effective macrocyclic-cation complexation [6]. It can be seen from Table 1 that macrocyclic cavity size is important in the interaction of Hg^{2+} , Ni^{2+} and Zn^{2+} cations with the ligands. For example, Ni^{2+} does not form a stable complex with 14-membered crown ether **L(1)** while it forms a stable 2:1 (M:L) complex with 16-membered crown ether **L(2)**. As seen from Table 1, **L(2)** formed stable complexes with many metal cations. On the contrary, **L(1)** forms stable complexes with less number of metal cations. This result can be explained by the flexibility of 16-membered crown ether **L(2)** with respect to 14-membered crown ether **L(1)**. As known, flexible macrocyclic ligands undergo structural changes during the complexation, hence, such ligands can form stable complexes with various metal cations.

Fluorescence spectra

Excitation at 345 nm of the ligands gives characteristic emission bands of pyrene between 370 and 450 nm. The fluoroionophoric properties of the ligands were investigated by fluorescence measurements in the presence of Al^{3+} , Zn^{2+} , Fe^{2+} , Fe^{3+} , Co^{2+} , Ni^{2+} , Mn^{2+} , Cu^{2+} , Cd^{2+} , Hg^{2+} and Pb^{2+} .

Figure 8a shows the effect of 10 M equivalent Al^{3+} , Pb^{2+} , Fe^{2+} , Hg^{2+} and Cu^{2+} on the fluorescence spectra of **L(1)**. There was a dramatic enhancement in the emission intensity of **L(1)** for the perchlorates of Al^{3+} and Pb^{2+} . This is probably a result of the hampered PET mechanism [13]. The interaction of the amino nitrogen atom with these cations causes the nitrogen atom to fail in donating an electron to the excited state of the pyrene ring. Thus, the addition of these cations causes the recovery of the fluorescence. Therefore, the reason of the enhancement in the fluorescence intensity may depend on the complexation with these cations. The effects of Zn^{2+} , Fe^{3+} , Co^{2+} , Ni^{2+} , Mn^{2+} and Cd^{2+} cations on the fluorescence spectra of **L(1)** are shown in Fig. 8b, where the fluorescence intensity of **L(1)** increased when 10 M equivalents of these cations were added except for Ni^{2+} . The effects of Ni^{2+} , Fe^{3+} and Mn^{2+} cations are minor. The most significant fluorescence enhancement was observed for Zn^{2+} . However, no stable complex formation was observed with these metal cations. Despite this, the observed fluorescence enhancement in the fluorescence spectra of **L(1)** can be explained by the above mentioned hampered PET mechanism.

We carried out spectrofluorimetric titrations for all metal cations with **L(1)** in acetonitrile-tetrahydrofuran (1:1). A regular fluorescence response was detected for Pb^{2+} with this ligand. A linear response of the fluorescence intensity as a function of Pb^{2+} concentration at 398 nm

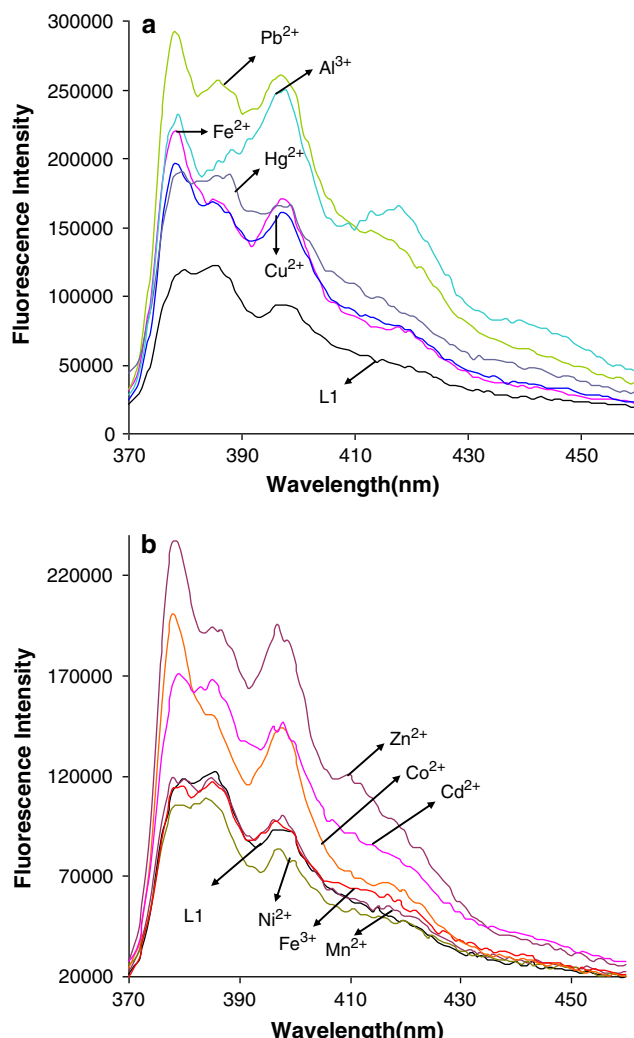


Fig. 8 The effect of metal cations on the fluorescence spectra of **L(1)** in acetonitrile-tetrahydrofuran solution (1:1). (Ligand concentration = 1.3×10^{-7} M. Metal perchlorate concentrations = 1.3×10^{-6} M, excitation at 345 nm, **a** for Al^{3+} , Fe^{2+} , Cu^{2+} , Hg^{2+} and Pb^{2+} . **b** for Zn^{2+} , Co^{2+} , Ni^{2+} , Mn^{2+} , Cd^{2+} and Fe^{3+})

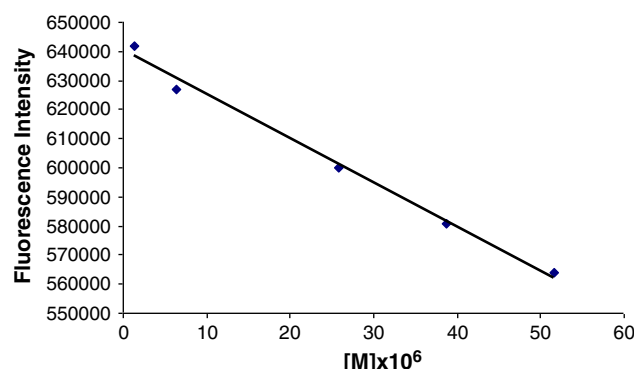


Fig. 9 The fluorescence intensity of **L(1)** versus the Pb^{2+} concentration for the spectrofluorimetric titration. Wavelength: 398 nm, Ligand concentration = 1.3×10^{-7} M

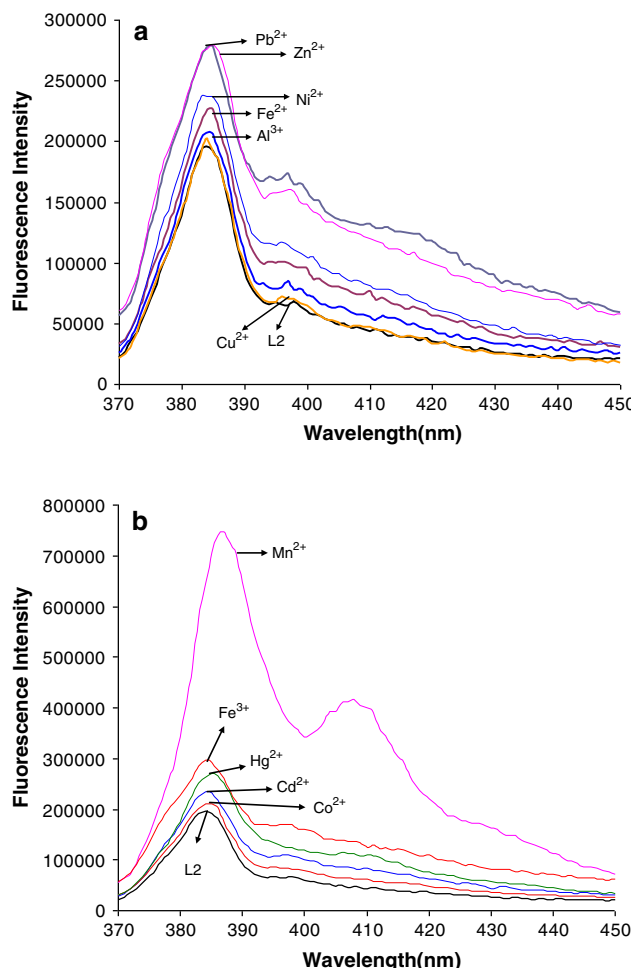


Fig. 10 The effect of metal cations on the fluorescence spectra of **L(2)** in acetonitrile-tetrahydrofuran solution (1:1). (Ligand concentration = 1.3×10^{-8} M. Metal perchlorate concentrations = 1.3×10^{-7} M, excitation at 345 nm, **a** for Al³⁺, Fe²⁺, Cu²⁺, Ni²⁺, Zn²⁺ and Pb²⁺. **b** for Hg²⁺, Co²⁺, Mn²⁺, Cd²⁺ and Fe³⁺

was observed from 1.3×10^{-6} to 5.2×10^{-5} M with linearly dependent coefficient $R^2 = 0.9928$ (Fig. 9). The detection limit calculated as three times the standard deviation of the blank signal was found to be 5.2×10^{-7} M.

Figure 10 shows the effect of metal cations on the fluorescence spectra of **L(2)**. The emission intensity of **L(2)** was enhanced upon the addition of 10 M equivalents of Zn²⁺, Pb²⁺, Al³⁺, Cu²⁺, Fe²⁺ and Ni²⁺ cations (see Fig. 10a). Especially, Zn²⁺ and Pb²⁺ caused a pronounced fluorescence increase. As seen from Table 1, Pb²⁺ forms the most stable complex with **L(2)**. These results can also be explained by the hampered PET mechanism as mentioned above. Figure 10b shows the effect of Fe³⁺, Co²⁺, Hg²⁺, Mn²⁺ and Cd²⁺ cations on the fluorescence spectra of **L(2)**. Although the spectrophotometric titration results did not show any stable complex formation with these cations, a fluorescence enhancement was observed in the

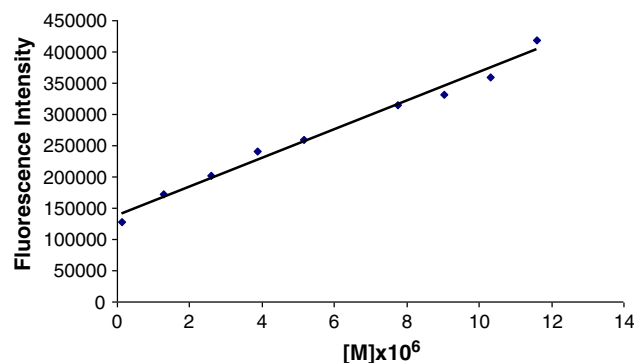


Fig. 11 The fluorescence intensity of **L(2)** versus the Ni²⁺ concentration for the spectrofluorimetric titration. Wavelength: 398 nm, Ligand concentration = 1.3×10^{-8} M

fluorescence spectra of **L(2)** with the excess concentration of these cations. The hampered PTE mechanism can enlighten these results depending on the interaction of the nitrogen donor atom in the crown ether with the mentioned metal cations.

Finally, we carried out spectrofluorimetric titrations for all metal cations with **L(2)** in acetonitrile-tetrahydrofuran (1:1). A regular fluorescence response was detected for Ni²⁺ with **L(2)**. A linear response of the fluorescence intensity as a function of Ni²⁺ concentration at 398 nm was observed from 1.3×10^{-7} to 5.2×10^{-6} M with linearly dependent coefficient $R^2 = 0.9856$ (Fig. 11). The detection limit calculated as three times the standard deviation of the blank signal was found to be 4.1×10^{-8} M.

Acknowledgments This work was supported by The Scientific and Technological Research Council of Turkey (TUBITAK).

References

1. Hama, H., Morozumi, T., Nakamura, H.: Novel Mg²⁺-responsive fluorescent chemosensor based on benzo-15-crown-5 possessing 1-naphthaleneacetamide moiety. *Tetrahedron Lett.* **48**, 1859–1861 (2007)
2. Xia, W.S., Schmehl, R.H., Li, C.J.: A highly selective fluorescent chemosensor for K⁺ from a bis-15-crown-5 derivative. *J. Am. Chem. Soc.* **121**, 5599–5600 (1999)
3. Chen, C.T., Huang, W.P.: A highly selective fluorescent chemosensor for lead ions. *J. Am. Chem. Soc.* **124**, 6246–6247 (2002)
4. Yan, Y., Hu, Y., Zhao, G., Kou, X.: A novel azathia-crown ether dye chromogenic chemosensor for the selective detection of mercury(II) ion. *Dyes Pigments* **79**, 210–215 (2008)
5. Shin, E.J.: Synthesis and fluorescence behavior of cation chemosensor based on azacrown ether fluorooionophore carrying styrylanthracene. *Bull. Korean Chem. Soc.* **27**, 1897–1899 (2006)
6. Izatt, R.M., Pawlak, K., Bradshaw, J.S., Bruening, R.L.: Thermodynamic and kinetic data for macrocycle interaction cations, anions and neutral molecules. *Chem. Rev.* **95**, 2529–2586 (1995)
7. Beklemishev, M.K., Dmitrienko, S.G., Isakova, N.V.: Macroyclic compounds in analytical chemistry. Wiley-Interscience, New York (1997)

8. Gunnlaugsson, T., Lee, T.C., Parkesh, R.: A highly selective and sensitive fluorescent PET (photoinduced electron transfer) chemosensor for Zn(II). *Org. Biomol. Chem.* **1**, 3265–3267 (2003)
9. Zhang, X.Y., Wang, Z.H., Yang, L.: A highly selective and sensitive fluorescent chemosensor for Zn^{2+} . *Chin. Chem. Lett.* **19**, 1240–1243 (2008)
10. Gou, X., Qian, X., Jia, L.: A Highly selective and sensitive fluorescent chemosensor for Hg^{2+} in neutral buffer aqueous solution. *J. Am. Chem. Soc.* **126**, 2272–2273 (2004)
11. Tamayo, A., Lodeiro, C., Escriche, L., Casabo, J., Covelo, B., Gonvales, P.: New fluorescence PET systems based on N_2S_2 pyridine-anthracene-containing macrocyclic ligands. Spectrophotometric, spectrofluorimetric, and metal ion binding studies. *Inorg. Chem.* **44**, 8105–8115 (2005)
12. Xu, X., Xu, H., Ji, H.F.: New fluorescent probes for the detection of mixed sodium and potassium metal ions. *Chem. Commun.* 2092–2093 (2001)
13. Valeur, B., Leray, I.: Design principles of fluorescent molecular sensors for cation recognition. *Coord. Chem. Rev.* **205**, 3–40 (2000)
14. Ji, H.F., Dabestani, R., Hettich, R.L., Brown, G.M.: Optical sensing of cesium using 1, 3-alternate calix[4]-mono-and di (anthrylmethyl)aza-crown-6. *Photochem. Photobiol.* **70**, 882–886 (1999)
15. Wang, H., Chan, W.H.: Cholic acid-based fluorescent sensor for mercuric and methyl mercuric ion in aqueous solutions. *Tetrahedron* **63**, 8825–8830 (2007)
16. Wang, S., Zhang, Q., Datta, P.K., Gawley, R.E., Leblanc, R.M.: Amphiphilic anthracyl crown ether. A Langmuir and langmuir-Schaefer films study. *Langmuir* **16**, 4607–4612 (2000)
17. Kubo, K., Sakurai, T.: Syntesis and fluorescence properties of N-(1-pyrenylmethyl)-18-azacrown-6. *Rep.Inst.Adv.Mat.* **10**, 85–87 (1996)
18. Collins, G. E.; Choi, L. S.: Fluorescent diaza crown ether sensitive to complexation, conformation and microenviroment. *Chem.Commun.*, 1135–1136 (1997)
19. Nakahara, Y., Kida, T., Nakatsuji, Y., Akashi, M.: Synthesis of double- armed lariat ether with pyrene moieties at each end of two sidearms and their fluorescence properties in the presence of alkali metal and alkaline earth metal cations. *J. Org. Chem.* **69**, 4403–4411 (2004)
20. Chang, J.H., Kim, H.J., Park, J.H., Shin, Y.K., Chung, Y.: Fluorescence intensity changes for anthrylazacrown ethers by paranagnetic metal cations. *Bull. Korean Chem. Soc.* **20**, 796–800 (1999)
21. Kwon, J.Y., Soh, J.H., Yoon, Y.J., Yoon, J.: Highly effective fluorescent sensor for Hg^{2+} in aqueous solution. *Supramol. Chem.* **16**, 621–624 (2004)
22. Minkin, V.I., Dubonosov, A.D., Bren, V.A., Tsukanov, A.V.: Chemosensors with crown ether-based receptors. *Arkivoc* 90–102 (2008)
23. Başoğlu, A., Parlayan, S., Ocak, M., Alp, H., Kantekin, H., Özdemir, M., Ocak, Ü.: Complexation of metal ions with the novel $N_2O_2S_2$ mixed donor macrobicyclic ligands carrying naphtyl fluorophore in acetonitrile-dichloromethane. *Polyhedron* **28**, 1115–1120 (2009)
24. Martin, J.W.L., Organ, G.J., Wainwright, K.P., Weerasuria, K.D.V., Willis, A.C., Wild, S.B.: Copper(I) complexes of 14- and 16-membered chelating macrocycles with trans-disposed pairs of imine-N and thioether-S donors: crystal and molecular structures of $[Cu(C_{18}H_{18}N_2S_2)]CF_3SO_3$ and $[Cu(C_{20}H_{22}N_2S_2)]CF_3SO_3$. *Inorg. Chem.* **26**, 2963–2968 (1997)